U.S. DEPARTMENT OF COMMERCE
Frederick B. Dent, Secretary
NATIONAL OCEANIC AND ATMOSPHERIC ADMINISTRATION
Robert M. White, Administrator
NATIONAL MARINE FISHERIES SERVICE

NOAA Technical Report NMFS SSRF-671

Coastal Upwelling Indices, West Coast of North America, 1946-71

ANDREW BAKUN

SEATTLE, WA
June 1973

For sale by the Superintendent of Documents, U.S. Government Printing Office
Washington, D.C. 20402

Coastal Upwelling Indices, West Coast of North America, 1946-71

ANDREW BAKUN[1]

ABSTRACT

A series of monthly indices of intensity of large-scale, wind-induced coastal upwelling at selected locations along the west coast of North America is presented for the period 1946 through 1971. The indices are based on calculations of offshore Ekman surface wind transport from monthly mean surface atmospheric pressure data. Summaries by quarter and by year are included.

The effect of using monthly mean pressure data is evaluated by comparison to a similar series of monthly means of transports computed 6-hourly over a 4½-yr period. The correlation between the two series at any particular location was found to be high. However, the slope of the regression line varies at different locations. Also values off southern California during summer may be amplified relative to other locations as a result of the discontinuity in the atmospheric pressure gradient caused by the coastal mountain range between the thermal low in the interior of southern California and the higher pressure offshore. The conclusion is that these series may be satisfactory indicators of temporal variations of upwelling at each location, but less satisfactory indicators of spatial distributions.

INTRODUCTION

Coastal upwelling can profoundly affect the physical environment of marine organisms. An extreme example is the "El Niño" of the Peru Current where high surface temperatures related to cessation of upwelling have apparently resulted in such dislocation of marine fauna as to have caused starvation of great numbers of guano-producing seabirds (Wooster, 1960). Perhaps even more important from a fishery standpoint is the role of upwelling in the cycle of organic production in the sea, both in transporting nutrient-rich deeper waters into the illuminated surface layers where they are available for production, and in providing virgin water which is sufficiently free from predators to allow accumulation of large phytoplankton blooms (Cushing, 1969). Estimates have run as high as Ryther's (1969) suggestion that upwelling areas comprising about one-tenth of 1% of the ocean surface may produce one-half of the world's harvestable fish supply. Evidently, some indication of fluctuations in the upwelling regime is extremely important to understanding fluctuations in marine populations. This report is an attempt to provide indices of intensity of coastal upwelling off western North America on time and space scales useful to fishery research in general, and to the MARMAP (Marine Resources Monitoring, Assessment and Prediction) program of the National Marine Fisheries Service in particular.

[1] Pacific Environmental Group, National Marine Fisheries Service, NOAA, Monterey, CA 93940.

METHOD

It is generally recognized that coastal upwelling in broad, diffuse eastern boundary currents such as the California Current and the eastern portion of the Gulf of Alaska Gyre is largely due to replacement from below of surface water transported offshore by the stress of the wind on the sea surface (Sverdrup et al., 1942, p. 501). Other possible mechanisms producing coastal up-

welling include upwarping of density surfaces within a geostrophic current (Stommel and Wooster, 1965) and cross-isobar onshore flow at the bottom due to bottom friction (Hsueh and O'Brien, 1971). However, these are more likely to be important in narrower, more intense flows than normally occur in the area covered by this report.

Our present understanding of surface wind transport is based on Ekman's (1905) theory. Under Ekman's assumptions of steady state motion, uniform wind, and infinite homogeneous ocean, the mass transport per unit width of ocean surface is directed 90 degrees to the right (in the Northern Hemisphere) of the direction toward which the wind is blowing and is related to the magnitude of the wind stress by the expression

$$M = \frac{\tau}{f} \tag{1}$$

where M is the mass transport resulting from a wind stress, τ, and f is the Coriolis parameter. This mass transport has come to be called the *Ekman transport*. The layer in which appreciable transport occurs is often referred to as the *Ekman layer* and extends from the surface to depths not exceeding 50 to 100 m. The bottom of the Ekman layer is sometimes identified with the bottom of the homogeneous wind-mixed zone.

Smith (1967) has shown that Yoshida's (1955) expression for the offshore transport in the early stage of coastal upwelling reduces to the Ekman transport expression if the stress is assumed constant. This leads to the conclusion that the Ekman theory gives a valid description of wind-driven offshore flow in the early nonequilibrium phase of upwelling as well as in the later steady-state phase.

The approach taken in generating the indices presented in this report has been to estimate the monthly mean wind stress on the sea surface at points near the coast, from this to compute the Ekman transport, and finally to resolve the component of Ekman transport perpendicular to the coast. The magnitude of the offshore component is considered an indication of the amount of water upwelled through the bottom of the Ekman layer to replace that driven offshore (Fig. 1). Negative values indicate onshore transport or convergence at the coast. Since accumulation of surface waters tends to cause downward displacement of the density structure in the coastal area, this situation is sometimes referred to as *downwelling*.

The basic input data is the wind field over the ocean. However, the distribution of sea-surface wind observations in the near coastal regions of the northeastern Pacific is uneven, both spatially and temporally. The number available for a given area during a given month is often insufficient to form a good estimate of the monthly mean stress on the sea surface. In order to construct a consistent series, use is made of the relationship in mid-latitude regions of wind to atmospheric pressure. Incorporating atmospheric pressure data increases the coverage in data-sparse areas and allows an understanding of the behavior of large-scale pressure systems to aid in providing continuity to the analysis of scattered observations. Therefore, winds derived from analyzed atmospheric pressure fields are used in the production of these indices.

Calculations

The computed values are based on monthly mean pressure fields prepared by Fleet Numerical Weather Central (FNWC). These data are available on a 63 by 63 point square grid which is superimposed on a polar stereographic projection of the Northern Hemisphere (Hughes, 1966). The mesh length is 200 nautical miles at lat. 60°N and decreases southward to about 144 nautical miles at lat. 20°N. The data were transferred to a 3-degree mesh length geographical (spherical coordinates) grid (Fig. 2) using Bessel's central difference formula.

First derivatives of the surface pressure at each grid point were estimated by taking the difference in pressure between the grid points to either side and dividing by the 6-degree angular mesh length. For example, the derivatives of the pressure at point "0" in Figure 3(a) would be approximated as

$$\frac{\partial P}{\partial \phi} \cong \frac{P_1 - P_2}{2h}; \quad \frac{\partial P}{\partial \lambda} \cong \frac{P_4 - P_3}{2h} \tag{2}$$

where ϕ and λ denote the northward and eastward angular coordinates, h is the 3-degree angular mesh length in radians and P_1 denotes the pressure at point "1", etc. The geostrophic wind was computed according to

$$u_g = -\frac{1}{f\rho_a R}\frac{\partial P}{\partial \phi}; \quad v_g = \frac{1}{f\rho_a R \cos\phi}\frac{\partial P}{\partial \lambda} \tag{3}$$

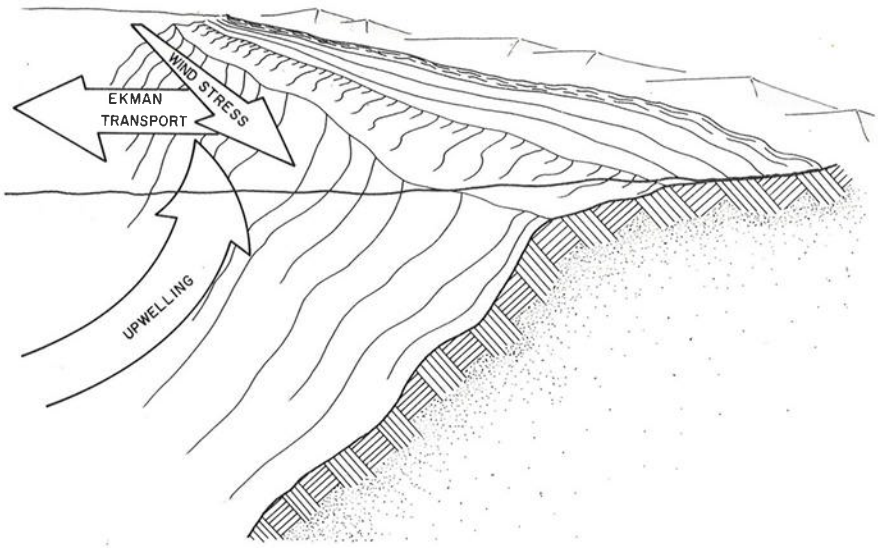

Figure 1.—A conceptual diagram of the coastal upwelling process. The coast of the continent is represented in cutaway view with the ocean to the left of the figure. Offshore transport in the surface Ekman layer due to stress of the wind parallel to the coast on the sea surface is replaced by upwelling from depth.

where v_g and u_g are the respective northward and eastward components of geostrophic wind velocity, f is the Coriolis parameter, ρ_a is the density of air and R is the mean radius of the earth. The density ρ_a was considered constant at 0.00122 g cm^{-1}. An estimate of the wind near the sea surface was formed by rotating the geostrophic wind vector 15 degrees to the left and reducing it by 30% as in Figure 3(b) to approximate frictional effects.

The sea-surface stress was then computed according to the classical square-law formula

$$\vec{\tau} = \rho_a C_d |\vec{v}| \vec{v} \qquad (4)$$

where $\vec{\tau}$ is the stress vector, ρ_a is the density of air, C_d is an empirical drag coefficient, $\vec{v}$ is the estimated wind vector near the sea surface with magnitude $|\vec{v}|$. A relatively high value, 0.0026, of the drag coefficient was used to partially offset the effect of using mean data. Finally, the Ekman transport was computed according to Equation (1). Except for the estimates of the pressure derivatives which necessarily differ because of the different grid format, this calculation procedure is the same as that used by Fofonoff (1960).[2] The offshore transport is determined by resolving the component perpendicular to a line drawn by visual estimation on a bathymetric chart along the dominant trend of a 200-mile segment of coastline centered near the grid point in question.

The indices generated by this method must be considered as indicative of rather large-scale coastal upwelling. The 6-degree gap across which the derivatives are measured as well as the scale of coastline resolution indicates a 100- to 200-mile scale as being appropriate for interpretation of the indices. Certainly, smaller scale upwellings could occur within a larger scale downwelling just as short-term upwellings might occur during a monthly period of average downwelling.

Pressure Data

The number of synoptic surface atmospheric pressure fields available at FNWC for each month during the period 1946-71 is variable. Because of the nonlinear dependence of stress on wind velocity (Equation 4), use of a variable sampling interval destroys the internal consistency of the time-series. For this reason monthly mean

[2] Fofonoff, N. P. 1960. Transport computations for the North Pacific Ocean-1958. Fish Res. Board Can., Manuscr. Rep. Ser. (Oceanogr. Limnol.) 80, 81 p. (Processed.)

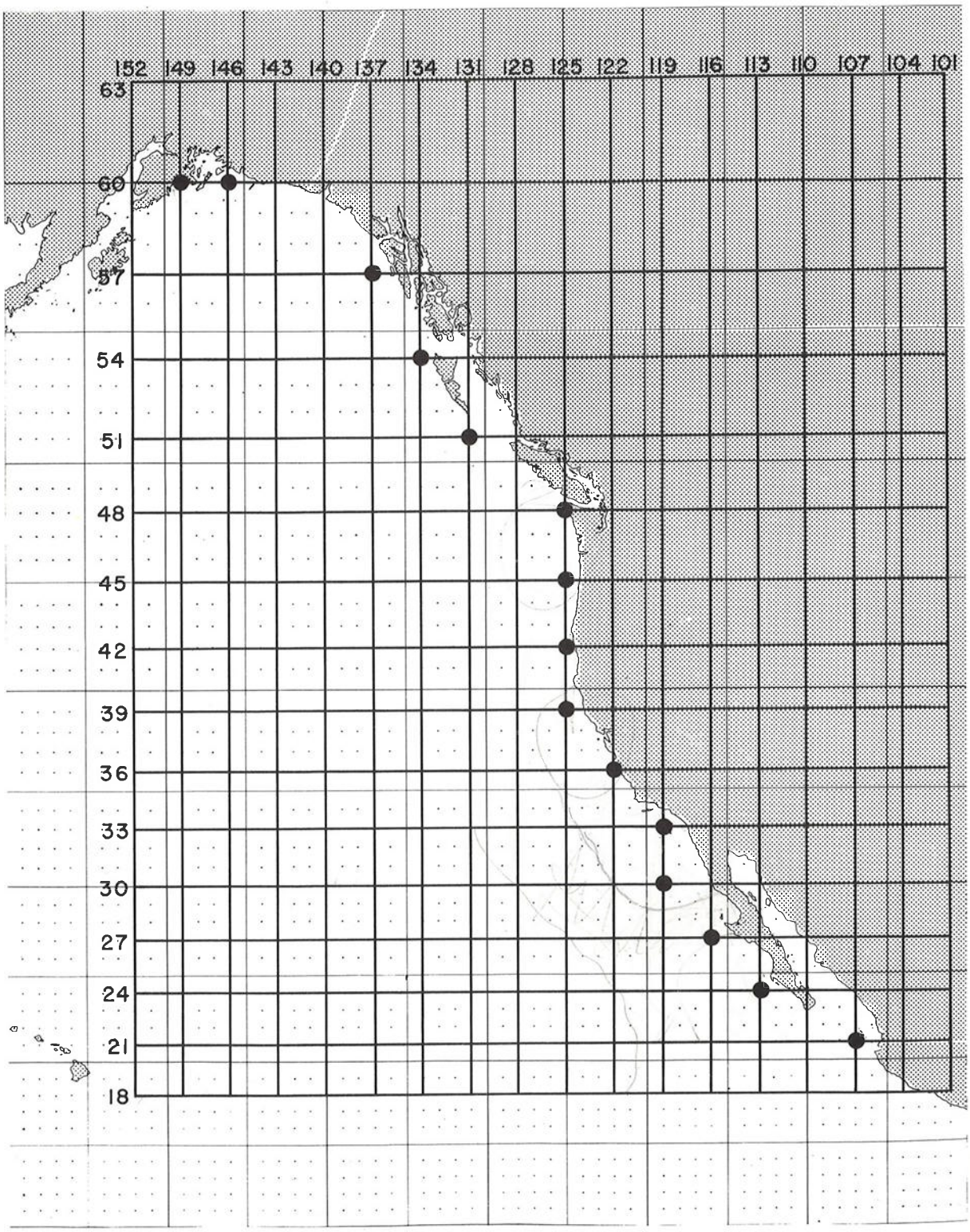

Figure 2.—Data grid. Intersections at which upwelling indices are computed are marked with large dots.

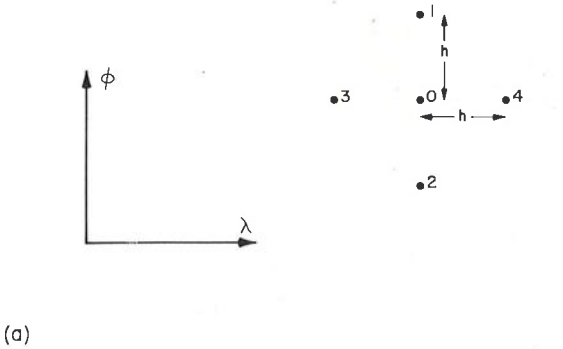

(a)

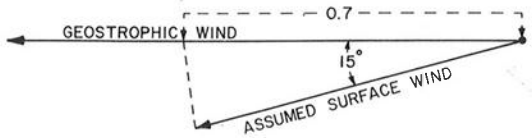

(b)

Figure 3.—(a) Configuration of data points used to form pressure derivatives. (b) Diagram showing the transformation of the geostrophic wind vector to form an estimate of the wind near the sea surface.

pressure fields were used as input data, thereby making best use of available data within each month while retaining a consistent sampling interval for computation of the stress. The effect of using monthly mean data on the absolute magnitude of the index at each location is discussed in the next section.

The monthly mean fields have been assembled by FNWC from, as far as was possible, 6-hourly (four per day) synoptic fields. Where this frequency was not available, twice per day where available or once per day fields were utilized. This decreased frequency occurs mainly in those years previous to 1963 when FNWC began to produce its own analysis. To extend the series back to 1946, FNWC has collected synoptic fields from the sources listed in Table 1.

Because of the different data sources and the expected trend toward increased detail in later pressure fields due to an expanded system of meteorological observations, care should be used in attempting to discern long-term trends in these upwelling indices. For example, it is difficult to determine how much of the decreased amplitude of the yearly cycle apparent at several of the locations during the earliest several years is real and how much is due to relative smoothing of the data in the earliest pressure fields. The intention has been to produce a series which will give a useful indication of the relative intensity of upwelling by month within any group of fairly contemporaneous years.

Effects of Monthly Mean Data on Calculated Results

Due to the nonlinear linkage of wind to stress (Equation 4) the value of the Ekman transport computed from monthly mean data will be small-

Table 1.—Sources of synoptic surface atmospheric pressure fields used by Fleet Numerical Weather Central in constructing monthly mean fields.

Time period	Source agency	Remarks
Jan. 1946-Mar. 1955	National Climatic Center Ashville, N.C.	Hand analysis of available reports; once per day.
Apr. 1955-Dec. 1959	National Center for Atmospheric Research Boulder, Colo.	National Meteorological Center analysis digitized at alternate gridpoints; twice per day.
Jan. 1960-June 1962	National Climatic Center Asheville, N.C.	Once per day.
July 1962-Dec. 1971	Fleet Numerical Weather Central, Monterey, Calif.	FNWC objective machine analysis. Certain gaps filled with NCC data; four times per day.

er than the monthly mean of Ekman transport computed at synoptic intervals by an amount depending upon the variance of the wind vector within the month. In order to evaluate this effect, a 54-mo series (January 1967 through June 1971) of monthly means of 6-hourly computations of offshore component of Ekman transport was generated for comparison with the corresponding values computed from monthly mean data. The results of the comparison are summarized in Table 2.

The high values of the correlation coefficients indicate quite linear relationships between the two sets of series. Thus the distortion introduced into the series at any particular location due to use of monthly mean data is mainly one of absolute magnitude. The relationship of each monthly value to the other monthly values at the location is affected only slightly. This indicates that the series computed from monthly mean data gives an indication of the monthly variations in intensity of upwelling nearly equivalent to that given by the corresponding series of monthly means of values computed each 6 hr.

However, Table 2 shows the slope of the regression line for the two series to be variable from one location to the other. This indicates a change with location in the amount of variability of the wind vector within a month. Thus the use of monthly mean data in conjunction with the nonlinear stress law (Equation 4) gives an erroneous impression of the relative magnitudes of offshore Ekman drift when different locations are compared. For this reason the indices tabulated in this report which are designed to indicate temporal variations at a particular location, should be used with caution as indicators of spatial distributions.

This distortion of the spatial distributions introduced by designing the computational method to minimize distortion of the time-series at each particular location can be illustrated by examining the long-term mean annual cycle of offshore Ekman transport computed in two different ways. Figure 4(a) is a time-series isogram of offshore component of Ekman transport for a long-term composite year computed from actual wind observations taken from the National Climatic Center's file of marine surface observations. The figure summarizes over 75,000 individual wind observations taken by ships at sea

Table 2.--Results of comparison of a 54-mo series of monthly means of offshore component of Ekman transport computed 6-hourly to the corresponding series computed from monthly mean data at the selected coastal grid-points.

Location	Rank correlation coefficient	Product-moment correlation coefficient	Slope of least-squares regression line
60°N,149°W	0.99	0.98	0.62
60°N,146°W	0.99	0.98	0.66
57°N,137°W	0.99	0.98	0.66
53°N,134°W	0.97	0.94	0.54
51°N,131°W	0.96	0.94	0.47
48°N,125°W	0.99	0.97	0.48
45°N,125°W	0.99	0.97	0.49
42°N,125°W	0.99	0.96	0.57
39°N,125°W	0.99	0.96	0.68
36°N,122°W	0.99	0.98	0.83
33°N,119°W	0.99	0.99	0.94
30°N,119°W	0.99	0.99	0.98
27°N,116°W	0.95	0.96	0.97
24°N,113°W	0.96	0.96	0.83
21°N,107°W	0.99	0.96	0.59

over the 20-yr period, 1948 through 1967, within the 1-degree squares shown in the accompanying coastline plot. The Ekman transport was computed for each wind observation and the offshore components were averaged by month for each coastal square. The drag coefficient used with these actual observed winds was 0.0013. Bakun (1971) demonstrated that the spatial distributions obtained in this manner agreed well with the mean annual cycle of sea-surface temperature distributions. Reference to the slopes of the regression lines in Table 2 indicates that since this drag coefficient is half that used with winds computed from monthly mean pressure fields to generate the indices tabulated in this report, rough numerical equivalence between the two transport sets should occur at about lat. 45°N.

Figure 4(b) is a similar isogram constructed from long-term mean monthly values for the same period of the indices derived from monthly mean pressure data. The locations at which the indices were calculated are marked on the accompanying coastline plot. Comparison with Figure 4(a) shows an extreme southward shift and intensification of the point of maximum indicated upwelling.

Figure 4(c) displays the data from Figure 4(b) after having been adjusted to the slopes of the re-

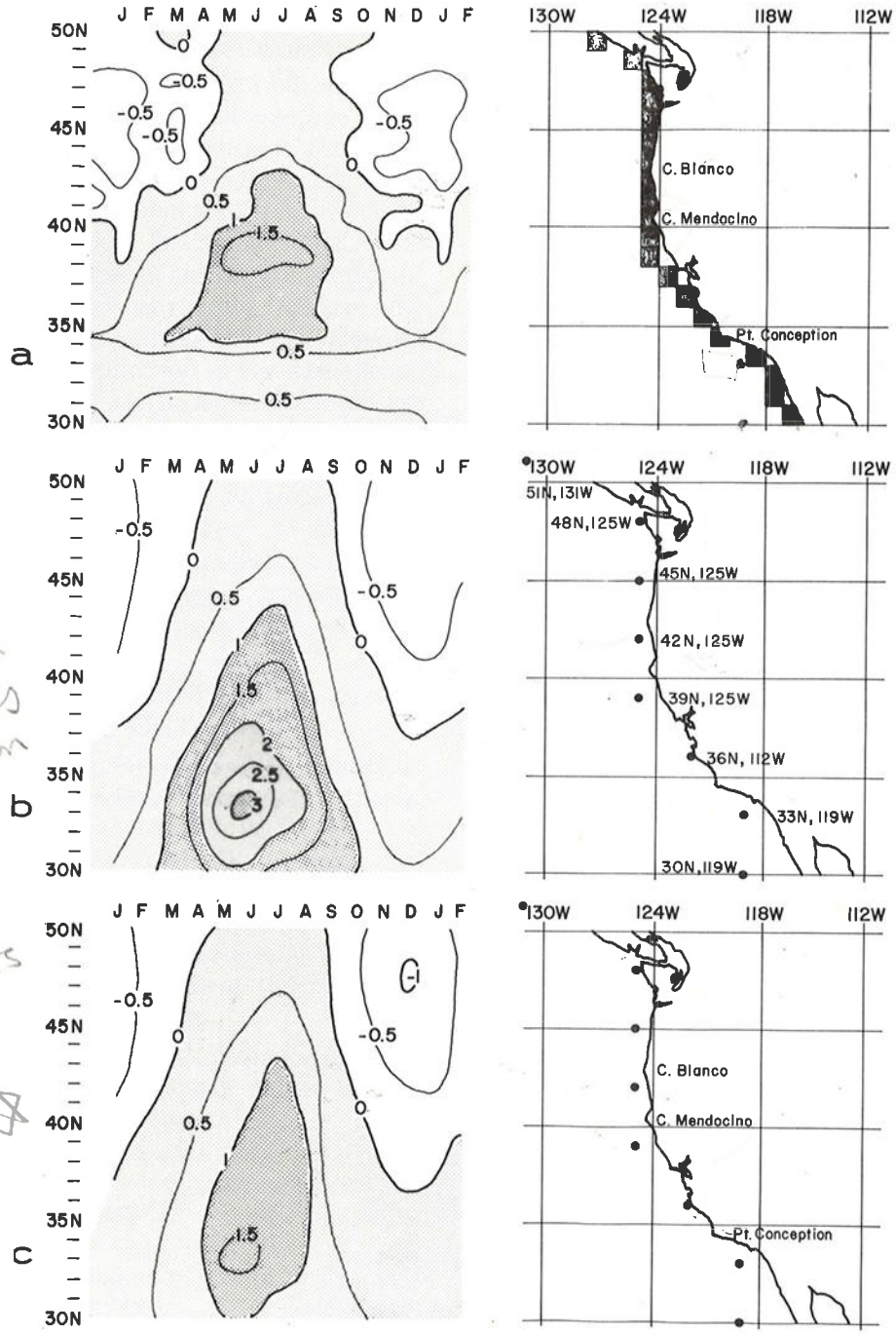

Figure 4.—(a) Long-term mean annual cycle of offshore Ekman transport composited from actual wind observations within the 1-degree squares indicated on the coastline drawing to the right. (b) Long-term mean annual cycle of offshore Ekman transport formed from upwelling indices computed from monthly mean atmospheric pressure data at points indicated by dots on the coastline drawing. (c) Values from Figure 4(a) after having been adjusted to the slopes of the regression lines in Table 2. Units are cubic meters per second per meter of coastline.

gression lines by multiplying each monthly value by 0.5 and by the reciprocal of the slope given in Table 2. The multiplication by 0.5 is necessary because the value of the drag coefficient used to construct Figure 4(a) is half that used for Figure 4(b) whereas the slopes in Table 2 were computed for two series with equal drag coefficients. Multiplication by the reciprocal of the slopes then serves to adjust the data so that the spatial variation in the underestimate of the monthly mean wind stress due to computation from monthly mean atmospheric pressure data as predicted in Table 2 is removed.

The magnitudes and spatial variations displayed in Figure 4(c) are more like those shown in Figure 4(a) than are those in Figure 4(b). Some smoothing of gradients in Figure 4(b) and (c) results from having data points at 3-degree intervals with each point incorporating data across a 6-degree area. This causes some loss in detail and displacement of contours relative to Figure 4(a) where data points are at 1-degree intervals and incorporate data restricted to a 1-degree square area. There remains however a definite shift of the maximum toward southern California in Figure 4(c) relative to Figure 4(a). A possible cause for this shift in maximum upwelling is described in the following section.

An Effect of Coastal Topography

During the summer an intense thermal low develops in the interior of southern California. Due to the 3-degree mesh length of the computation grid, the meridional component of the geostrophic wind at a coastal gridpoint is computed (Equation 2) from a continuous constant pressure gradient between an offshore gridpoint and one on the continent (dashed line in Fig. 5). However, the southern California coastal mountain range causes a discontinuity in this pressure gradient such that the gradient actually in equilibrium with the geostrophic wind (solid line in Fig. 5) may be less than that used in the computations. This leads to an overestimation of the geostrophic wind that in turn leads to an overestimation of the upwelling index. The assumption made in presenting these series as indicators of time variations of intensity of coastal upwelling is that the actual pressure gradient at the coast varies in rough proportion to the total onshore-offshore pressure difference which is used in the computations.

MEAN YEARLY CYCLE OF INDICATED UPWELLING

Having been designed to give a consistant indication of temporal variations at each particular

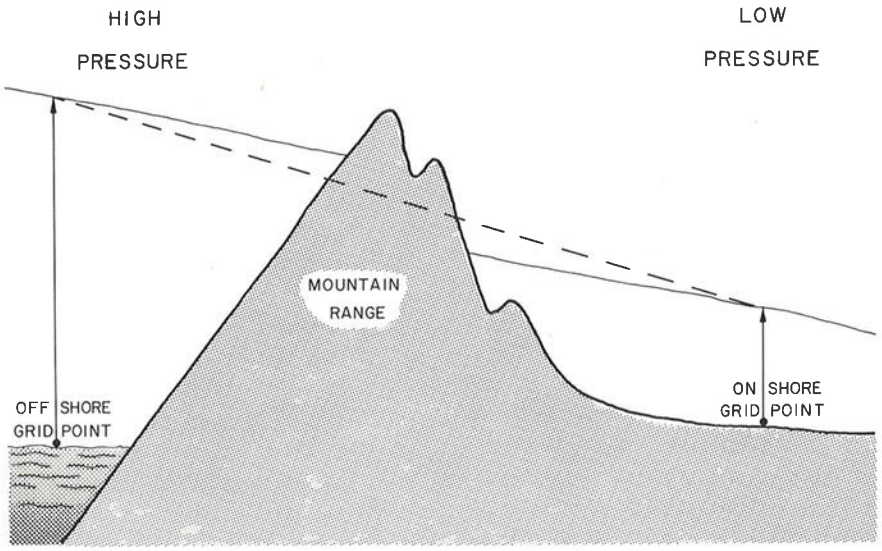

Figure 5.—Height of a constant pressure surface. The slope of the dashed line indicates the assumed gradient used in the calculations. The slope of the solid line indicates the lesser gradient which may exist in reality.

Table 3.—Mean monthly values of the indices for the 20-yr period, 1948-1967. Units are cubic meters per second per 100 m of coastline.

	Jan.	Feb.	Mar.	Apr.	May	June	July	Aug.	Sept.	Oct.	Nov.	Dec.
60°N,149°W	-138	- 86	-46	-11	0	6	6	6	- 3	-26	-73	-109
60°N,146°W	-180	-103	-48	-12	- 2	6	5	3	- 9	-34	-94	-129
57°N,137°W	-212	-117	-51	-24	-11	0	1	-6	-29	-88	-140	-163
54°N,134°W	- 97	- 68	-27	-20	-10	1	3	-1	-23	-82	- 98	- 91
51°N,131°W	- 64	- 36	-12	- 5	4	15	16	12	- 3	-40	- 58	- 57
48°N,125°W	- 90	- 47	-21	0	18	25	34	22	4	-39	- 88	-100
45°N,125°W	- 94	- 47	-15	9	34	48	74	50	16	-20	- 73	- 93
42°N,125°W	- 67	- 28	3	33	79	103	132	91	36	0	- 42	- 57
39°N,125°W	- 13	9	36	69	124	168	182	139	63	20	- 7	- 12
36°N,122°W	11	35	80	121	203	239	198	183	94	49	12	7
33°N,119°W	19	48	120	178	282	312	231	212	137	76	22	10
30°N,119°W	56	77	116	141	199	199	143	142	129	103	65	54
27°N,116°W	71	93	119	148	202	195	114	105	110	106	74	63
24°N,113°W	51	74	93	116	143	129	48	44	49	69	52	39
21°N,107°W	18	39	97	100	87	39	3	5	-14	-15	8	8

location, this set of indices may be admirably suited for describing the spatial variations of timing and duration of upwelling. In Table 3 are listed the long-term monthly mean values of the indices for the 20-yr period, 1948-67. Figure 6 displays plots of these values.

The period of maximum values of the indices is earliest to the south, becoming progressively later in the year with distance to the north. At lat. 21°N the peak is in April. Off the coast of Baja California the peak is in May. A June peak occurs off southern and central California. North of San Francisco the peak is generally in July, with a slight shift back to June at the northern extremity of the Gulf of Alaska.

From the southern tip of Baja California northward to Monterey Bay the mean values of the indices indicate upwelling throughout the year. Northward from San Francisco the season of indicated upwelling becomes progressively restricted, lasting March through October off northern California, April through September off Oregon, May through August off northern Vancouver Island, finally narrowing at lat. 57°N to a scarcely significant positive value of the index during July.

Tabulations of the deviations from these long-term mean values accompany the tabulations of the values of the indices in the Appendix. Graphical plots of both the anomalies and the values of the indices are included.

DISCUSSION

Detailed analysis and interpretation of the time-series plots contained in the Appendix is beyond the scope of this report. However, it may be useful to point out several examples and to speculate briefly upon possible consequences.

Accompanying the plots of the monthly indices for each location are tables of quarterly and annual averages. The following three examples are each illustrative of phenomena occurring basically on one of these three different time-scales. As it happens, the first two concern negative values of the index. Negative values of the index indicate accumulation of wind-transported surface waters at the coast and resulting downwelling.

Short-Term Intense Convergences in the Northern Gulf of Alaska

A glance at the first chart in the Appendix reveals an extreme negative spike in the upwelling index at lat. 60°N, long. 149°W during February 1950. In this case, the indicated convergence is over 4½ times the 20-yr mean value for February. It is interesting to speculate upon the effect of such an anomaly on the density structure of the northern portion of the Alaskan Gyre.

If the given numerical value is accepted as an estimate, we find for February 1950 an anomalous onshore flow of nearly 300 m^3/sec along each

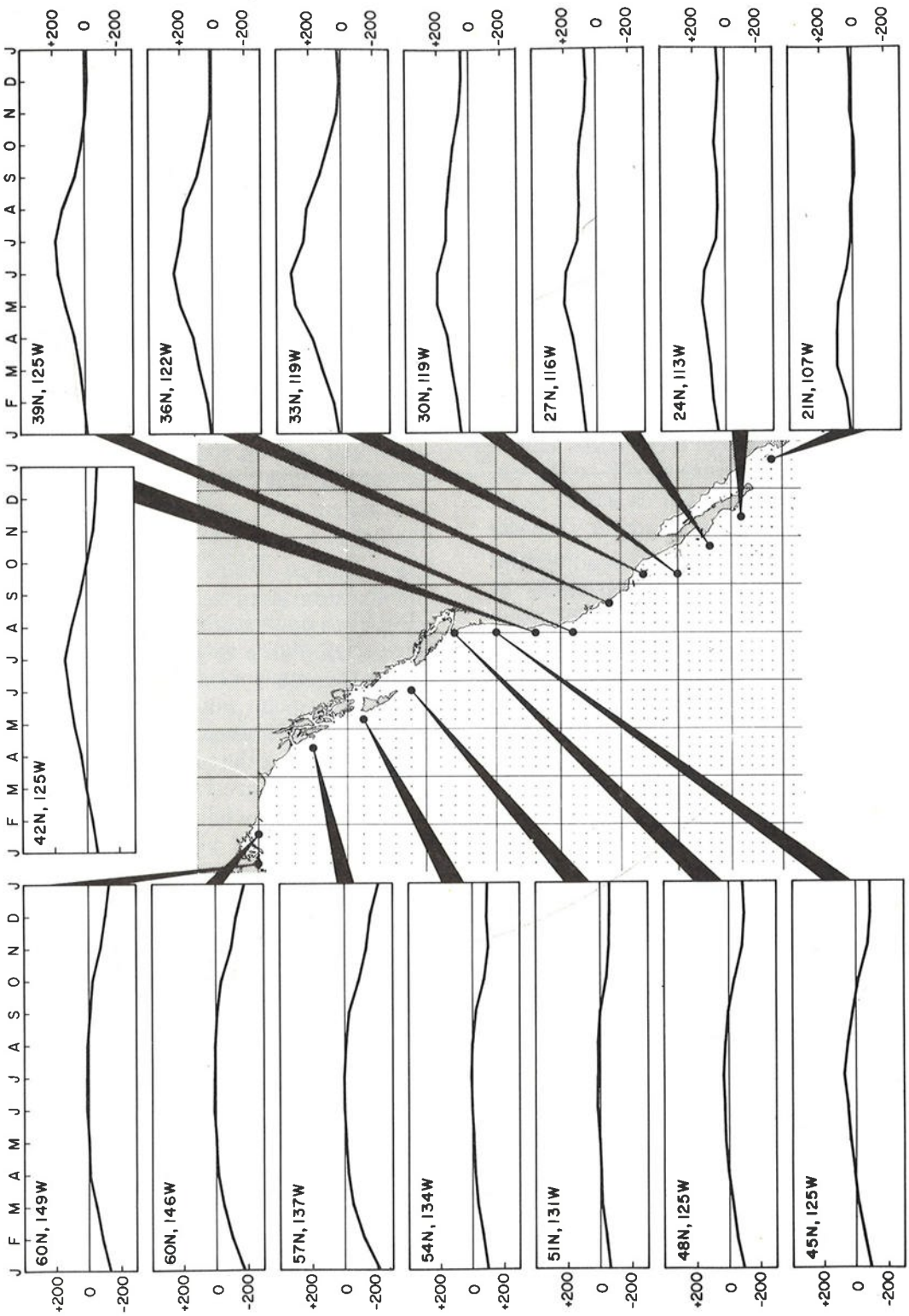

Figure 6.—Mean monthly values of the computed upwelling indices for the 20-yr period, 1948 through through 1967 (m^3 sec^{-1}/per 100 m).

100 m of coastline. Assuming this flow accumulates within a zone extending 300 km offshore, this represents for the 1-mo period a lens of excess surface water about 24 m thick. If the flow away from the coast which must balance this accumulation occurs below the pycnocline the result is a downward shift of the upper density structure an average of 24 m over the shoreward 300 km. Such a shift implies an extreme increase in baroclinicity in this already highly baroclinic area, tending to accelerate the westward geostrophic flow along the northern boundary of the Gulf of Alaska.

The striking negative anomalies for the same month in charts of the index at lat. 60°N, long. 146°W and at lat. 57°N, long. 137°W indicate that this feature existed over the major portion of the northern Gulf of Alaska coastline. This wide geographical extent justifies such a two-dimensional treatment as presented in the previous paragraph. It also indicates a possibly far-reaching effect on the marine environment of this region.

Several similar short-term intense negative values of the index appear in the charts at other times. In each case the major pulse is confined to only one monthly value but has spatial coherence in the Northern Gulf. Most impressive along with February 1950 just discussed are the months of January during the years 1959, 1966, and 1971. January 1971 differs from the others in that the absence of a strong anomaly at lat. 57°N, long. 135°W indicates a lesser eastward extent of the feature.

Periods of Intense Winter Convergence off Washington and Oregon

The monthly charts of the index at lat. 45°N, long. 125°W indicate the periods of December 1957 through February 1958 and January through March 1961 as having been intervals of extreme convergence of wind-drifted surface waters at the coast. Winter of 1958, in particular, exhibits a striking anomaly in the charts for locations extending from lat. 51°N to lat. 39°N. These periods differ from the intense convergences previously described for the more northerly region in containing several successive months of anomalously large negative values of the index rather than a single extreme month and are highly evident in the charts of quarterly summaries presented in the appendix. The effect of this apparent downwelling at the coast upon the density structure would be to accelerate northward flow or to decelerate southward flow. Either situation would favor an anomalous warm advection.

Long-Term Groupings of Mean Yearly Values

In examining these data for long-term or regional trends it is sometimes helpful to filter out some of the shorter term variability by means of annual averages. For example the charts of mean yearly values indicate anomalously high mean annual upwelling throughout the most recent 8-yr period, 1964 through 1971, from Cape Blanco to San Diego (lat. 42°N to lat. 33°N). In contrast, along Baja California (lat. 30°N to lat. 24°N) strikingly low anomalies are indicated for the 4 successive years, 1965 through 1968.

The period 1955 through 1959 has anomalously high values from the Los Angeles Bight to the southernmost point covered by the grid (lat. 33°N to lat. 21°N). In fact, the anomalously high values during this period extend all the way north to the Straits of Juan de Fuca (lat. 48°N) if the year 1958 which is anomalously low in the more northern area is left out. The low yearly mean values for 1958 are largely due to the extremely low first quarter value previously discussed.

Low annual absolute values of the indices are found for the first 4 yr of the series (1946-49) at nearly all locations. As previously mentioned this may be due, at least in part, to relatively sparse data coverage in the early years leading to some smoothing of the gradients used in the computations.

Conclusion

Anomalies of the type discussed may have important marine biological consequences. Vertical displacements of the thermocline due to intense convergences or divergences such as that indicated for February 1950 may affect the depth on the continental shelf where groundfish are located. Anomalous upwellings and downwellings undoubtably affect productivity and the concentrations of primary producers and zooplankton.

They may also affect recruitment and distribution of fishery resources, particularly where the anomaly is of longer term or recurs in successive years.

In view of these possibilities it is hoped that biologists will find the indices presented here to be convenient and suitable for incorporation into studies of the dynamics of biological distributions, and that empirical associations may lead to ecological hypotheses and finally to experiments which can verify both the hypotheses and the indices presented in this report. Finally, although this work was directed primarily toward developing a tool for biological and fisheries research, it is suggested that these indices may find applications in such fields as coastal oceanography, fog research, and studies of climate and weather of coastal regions.

ACKNOWLEDGMENTS

Invaluable discussion and advice was provided by James H. Johnson, Gunter R. Seckel, and Douglas R. McLain of the Pacific Environmental Group, National Marine Fisheries Service, NOAA, throughout this project, from its conception through the completion of the manuscript.

Atmospheric pressure data and electronic computing and plotting facilities were provided by the U.S. Navy, Fleet Numerical Weather Central.

LITERATURE CITED

BAKUN, A.
1971. Climatology of upwelling off California. (Abstract.) (030), AGU 1971 Fall Annu. Meet. EOS-Trans. Am. Geophys. Union 52(11):850.

CUSHING, D. H.
1969. Upwelling and fish production. FAO Fish. Tech. Pap. 84, 40 p.

EKMAN, V. W.
1905. On the influence of the earth's rotation on ocean currents. Ark. Mat. Astron. Fys. 2, 11:1-52.

HSUEH, Y. and J. J. O'BRIEN.
1971. Steady coastal upwelling induced by an alongshore current. J. Phys. Ocean. 1:180-186.

HUGHES, R. E.
1966. Computor products manual. Fleet Num. Weather Facil., Tech. Note 21, 301 p.

RYTHER, J. H.
1969. Photosynthesis and fish production in the sea. Science (Wash., D.C.) 166:72-76.

SMITH, R. L.
1967. Note on Yoshida's (1955) theory of coastal upwelling. J. Geophys. Res. 72:1396-1397.

STOMMEL, H., and W. S. WOOSTER.
1965. Reconnaissance of the Somali Current during the southwest monsoon. Proc. Natl. Acad. Sci. 54:8-13.

SVERDRUP, H. U., M. W. JOHNSON, and R. H. FLEMING.
1942. The oceans, their physics, chemistry, and general biology. Prentice-Hall, New York, 1087 p.

WOOSTER, W. S.
1960. El Niño. Rep. Calif. Coop. Oceanic Fish. Invest. 7:43-45.

YOSHIDA, K.
1955. Coastal upwelling of the California coast. Rec. Oceanogr. Works Jap. 2(2):8-20.